Nontraumatic Intracranial Hemorrhage

5

Pamela W. Schaefer and Myriam Edjlali

Abstract

Spontaneous ICH is usually intraparenchymal or subarachnoid in location. Intraparenchymal hemorrhages, encompassing lobar or centrally located hematomas, have diverse underlying causes, with cerebral amyloid angiopathy, characterized by lobar hemorrhage, being the most common. Hypertension is the second most common cause with a predilection for the basal ganglia, pons, and cerebellum. Subarachnoid hemorrhage is linked to aneurysm rupture in 85% of cases. Other relatively common causes of spontaneous intracranial hemorrhage include hemorrhagic conversion of ischemic infarction, cerebral arteriovenous malformations, dural arteriovenous fistulas, venous sinus thrombosis, cavernous malformations, reversible cerebral vasoconstriction syndrome, coagulopathy, and underlying tumors.

Computed tomography followed by CT angiography is used for initial assessment of spontaneous ICH. However, MRI is more sensitive than CT for the detection of ICH and plays an important role in their etiology characterization. In this paper, the authors present a logical approach to imaging spontaneous intracranial hemorrhage including identifying prognostic factors, determining etiology, and establishing treatment.

Keywords

Intracranial hemorrhage · Intraparenchymal hemorrhage Subarachnoid hemorrhage · Microhemorrhage · Lobar hemorrhage · Basal ganglia hemorrhage cerebral amyloid angiopathy · Hypertensive hemorrhage Leptomeningeal hemosiderosis · Cerebral venous sinus thrombosis · Cerebral arteriovenous malformation

Learning Objectives

- To know the CT and MRI protocols used to detect and characterize intracranial hemorrhage.
- To understand the key imaging features of intracranial hemorrhage on CT and MRI including signs that determine prognosis.
- To know the differential diagnosis of nontraumatic ICH based on hemorrhage location and patient demographics.
- To understand the key imaging characteristics of the major causes of nontraumatic intracranial hemorrhage.
- To know how to triage patients with nontraumatic intracranial hemorrhage for further imaging and treatment.

5.1 Introduction and Imaging Protocol

Nontraumatic intracranial hemorrhage accounts for up to 15% of all strokes and has an incidence of 10–30/100,000. Morbidity and mortality are higher for hemorrhagic stroke compared to ischemic stroke with a 1-year survival of approximately 30%. The incidence increases with age and is higher in males than females. The most common risk factor is hypertension. Other factors such as diabetes, anticoagulant therapy, dyslipidemia, and alcohol abuse also play an impor-

P. W. Schaefer
Radiology Department, Massachusetts General Hospital, Boston, MA, USA
e-mail: pschaefer@partners.org; pschaefer@mgh.harvard.edu

M. Edjlali (✉)
Radiology Department, Garches and Ambroise Paré Hospital, BioMaps, Paris Saclay University, Paris, France
e-mail: myriam.edjlali@aphp.fr

J. Hodler et al. (eds.), *Diseases of the Brain, Head and Neck, Spine 2024-2027*, IDKD Springer Series,
https://doi.org/10.1007/978-3-031-50675-8_5

tant role. Prognosis depends on the severity of risk factors as well as complications of ICH such as the development of hydrocephalus, brain herniation, or vasospasm.

The initial radiological assessment typically includes a CT scan followed by CT angiography to detect acute hemorrhages and their causes. While MRI is less common in the acute phase, it offers high sensitivity, particularly when performed shortly after symptom onset (<24 h).

When investigating intracranial bleeding causes after excluding intracranial aneurysms with CT angiography, MRI proves valuable for identifying the underlying factors. The imaging protocol should encompass DWI for the detection of associated ischemia, ideally 3D FLAIR to minimize CSF artifact for detection of edema and subarachnoid hemorrhage, SWI imaging for chronic microbleeds and hemosiderosis from amyloid angiopathy, time-of-flight MRA (possibly with gadolinium enhancement for distal arterial stenosis), and dynamic MRA to assess arteriovenous shunts. An arterial spin labeling sequence (ASL) is highly useful for detecting increased cerebral blood flow (CBF), which may indicate tumors or vascular shunts. ASL, being insensitive to blood components, is the preferred perfusion sequence for analyzing hemorrhagic components. 3D T1-weighted sequences with and without contrast to assess for an underlying mass lesion should also be obtained.

5.2 Subarachnoid Hemorrhage

5.2.1 Overview

Subarachnoid hemorrhage (SAH) is the third most common subtype of stroke. The incidence of SAH has decreased over the past few decades, possibly due to factors like lifestyle changes, such as quitting smoking and better management of hypertension. Around a quarter of SAH patients don't survive before they can be admitted to the hospital. However, the overall outcomes are better for those who make it to the hospital, although they still face an increased risk of long-term neuropsychiatric issues like depression. This condition continues to have a significant impact on public health, as the average age of onset is in the mid-50 s, leading to many years of reduced quality of life [1]. Subarachnoid hemorrhage (SAH) is defined as blood in the cerebrospinal fluid contained in the basal cisterns and the subarachnoid spaces of the cerebral hemispheres, located between the arachnoid mater and the pia mater. Nontraumatic subarachnoid hemorrhage (SAH) has an annual incidence of 9 per 100,000 individuals. It is a rare yet serious event, with an estimated mortality rate of 40% within the first 48 h. In 85% of cases, it is associated with the rupture of an intracranial aneurysm (Fig. 5.1). If SAH is suspected, cerebral imaging should be

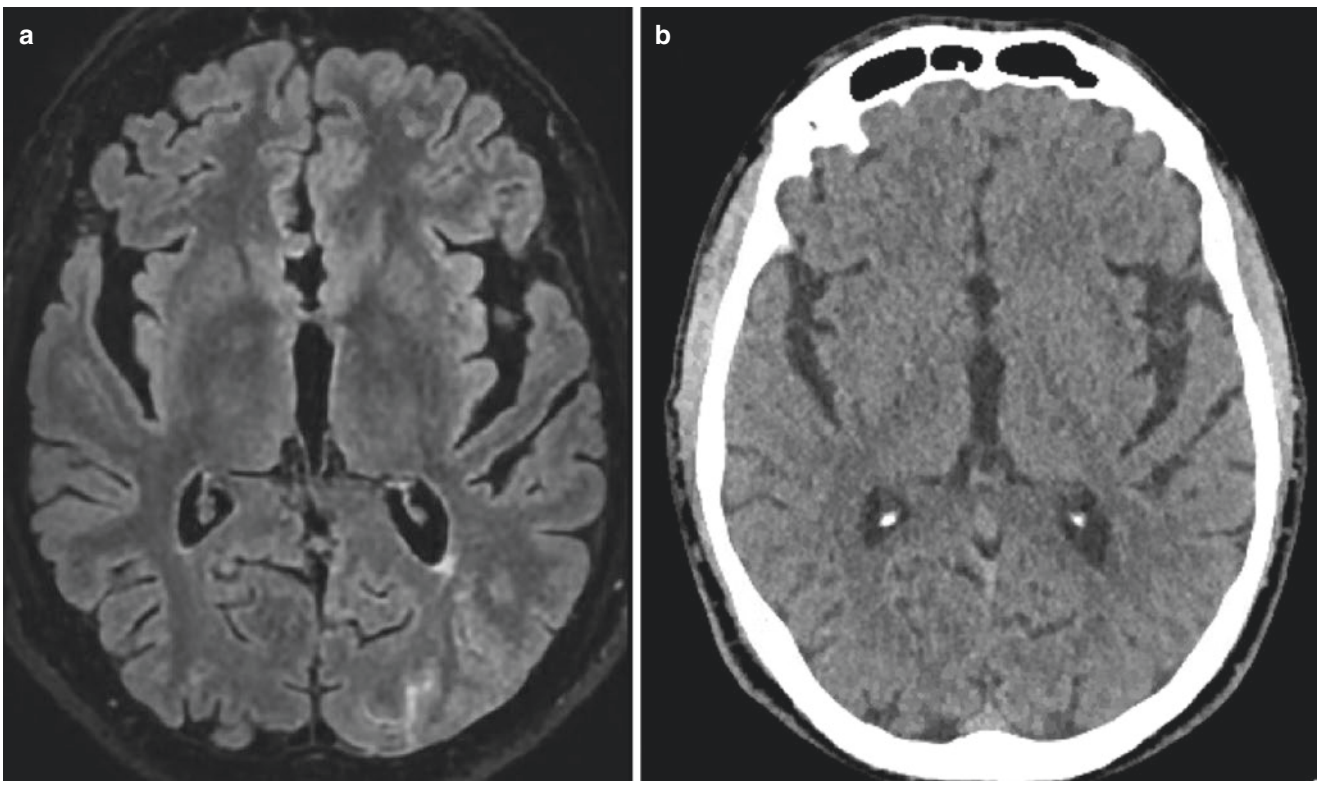

Fig. 5.1 Enhanced FLAIR sensitivity (**a**) in detecting subarachnoid hemorrhage compared to a negative CT scan (**b**) acquired on the same day, 5 days after the onset of severe headaches in a 45-year-old male

performed urgently to confirm the diagnosis, identify any complications, and investigate its cause. During the early phase, within the first 24 h, a CT scan of the brain combined with CT angiography of the circle of Willis is the recommended examination for a positive SAH diagnosis and for etiological diagnosis to detect an intracranial aneurysm. A diagnosis of subarachnoid hemorrhage (SAH) can be established through a CT scan when an unenhanced hyperdensity is observed within the subarachnoid spaces, typically involving the basal cisterns, interhemispheric sulci, and lateral sulci. If the patient's clinical condition allows, cerebral MRI may be considered. The FLAIR sequence is more sensitive than a CT scan in demonstrating subarachnoid hemorrhage (Fig. 5.2), especially after 48 h from symptom onset, and has a higher sensitivity for the etiological diagnosis of sulcal hemorrhages. In addition, combining FLAIR and SWI represents the most effective protocol for detecting subarachnoid hemorrhage (SAH) in the acute, subacute, or late phases of the hemorrhage. If these examinations yield normal results but clinical suspicion remains high, a lumbar puncture should be performed.

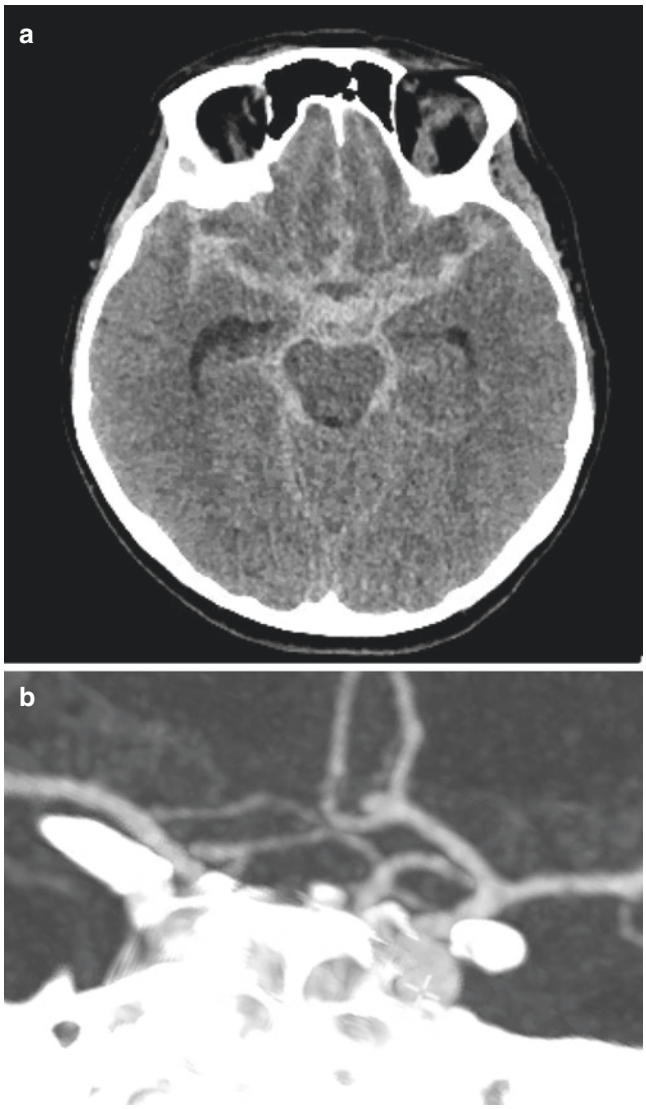

Fig. 5.2 A 62-year-old female with severe headaches. Noncontrast CT (**a**) reveals spontaneous hyperdensity in the subarachnoid spaces, indicative of an acute subarachnoid hemorrhage, along with initial ventricular dilation suggesting the onset of hydrocephalus. CT Angiography (**b**) identifies the source of the bleeding as a ruptured aneurysm of the anterior communicating artery

5.2.1.1 Main Etiologies of a SAH

Subarachnoid hemorrhage (SAH) [1] can result from various underlying causes, with the primary etiologies falling into several categories [2]:

1. **Aneurysm** [3]: Aneurysms, which are weakened and bulging areas in the walls of blood vessels, are a leading cause of SAH. When an aneurysm ruptures, it releases blood into the subarachnoid space, leading to SAH. The most common aneurysms associated with SAH are saccular aneurysms found in the circle of Willis.
2. **Dural AVF (Arteriovenous Fistula) or cortical venous thrombosis** [4]: Abnormal connections between arteries and veins within the dura mater (the membrane surrounding the brain) known as dural arteriovenous fistulas or cortical venous thrombosis can also result in SAH. These conditions disrupt normal blood flow, increasing the risk of hemorrhage.
3. **RCVS (Reversible Cerebral Vasoconstriction Syndrome)** [5]: RCVS is a relatively rare but important cause of SAH. It involves the sudden narrowing of cerebral blood vessels, which can lead to severe headaches and, in some cases, SAH. The vasoconstriction is typically reversible with time.
4. **Other**: Nontraumatic subarachnoid hemorrhage (SAH) can also stem from less typical sources, including endocarditis leading to mycotic aneurysm formation, vasculitides, amyloid angiopathy [6], tumors, arteriovenous malformations, bleeding disorders, and infections (Fig. 5.3). In certain instances, pinpointing the exact underlying cause may pose a diagnostic challenge, necessitating a comprehensive evaluation. Understanding the underlying etiology of SAH is crucial for appropriate management and treatment decisions, as each cause may necessitate distinct diagnostic workup and therapeutic approaches.

5.2.1.2 How Can I Determine Which of the Multiple Intracranial Aneurysms Has Bled During a SAH Assessment?

In cases where multiple intracranial aneurysms are present, accounting for 15 to 20% of cases, it is essential to prioritize treatment for the ruptured aneurysm before addressing the others. While the distribution of the SAH may provide some clues about the ruptured aneurysm, it is often insufficient for a definitive conclusion.

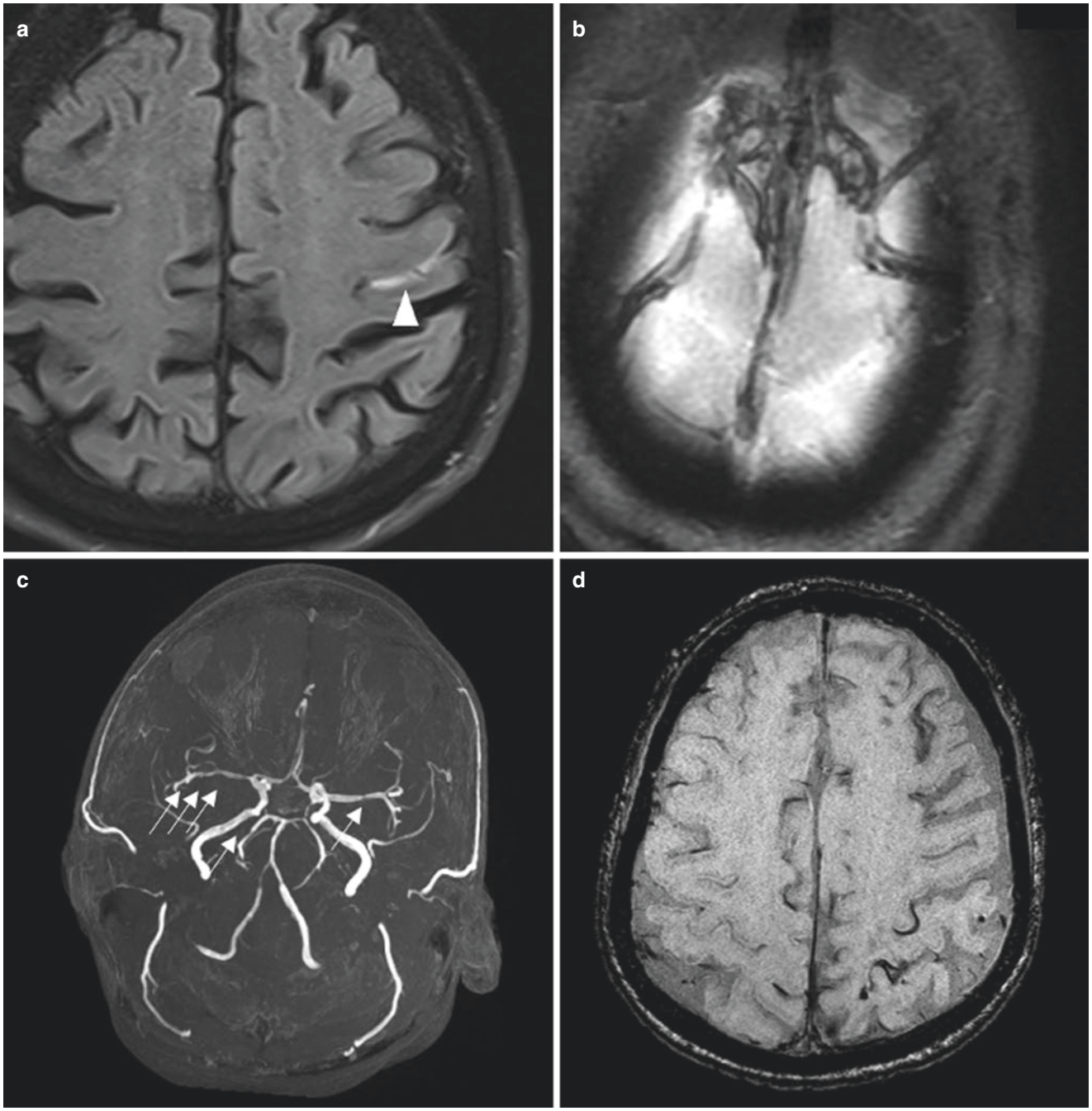

Fig. 5.3 Spontaneous subarachnoid hemorrhage at the vertex (**a**, head arrow) and various non-aneurysmal causes, including cerebral sinus and cortical vein thrombosis (**b**), reversible cerebral vasoconstriction syndrome (**c**), and amyloid angiopathy (**d**)

One indicator to consider is the irregular, scalloped "blister-like" appearance of the aneurysm wall, which suggests fissuring or rupture. Other indicators are size over 6 mm, interval grow from a prior scan.

Furthermore, on 3 Tesla MRI with 3D T1-weighted FSE sequences and gadolinium enhancement, circumferential enhancement of the aneurysm wall is believed to be a sign favoring unstable aneurysms (Fig. 5.4). These are more commonly observed in cases of aneurysms that have ruptured compared to aneurysms within the same patient that have not yet ruptured [7].

5.2.1.3 When Dealing with a Cisternal SAH and a Negative CT Angiogram, Three Possibilities Should Be Considered

1. **Undetected arterial abnormality**: It is possible that an arterial abnormality exists but has not been detected.

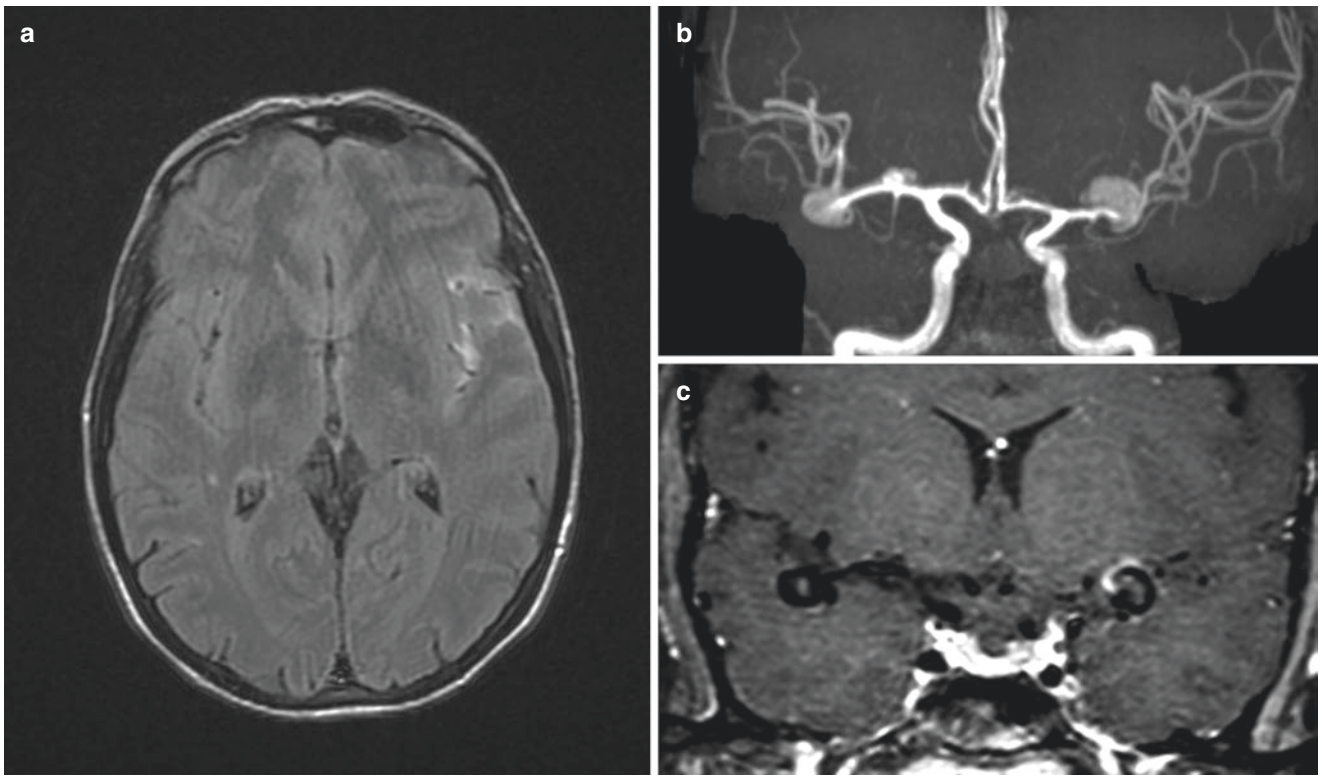

Fig. 5.4 Spontaneous subarachnoid hemorrhage (**a**) resulting from a ruptured aneurysm in a 50-year-old female with multiple aneurysms (angioMR 3D time-of-flight, **b**). The ruptured aneurysm is the only one exhibiting arterial wall enhancement in vessel wall imaging (**c**), confirming its association with the site of bleeding as seen in the FLAIR image

Small intracranial aneurysms in the posterior circulation can be challenging to identify on standard imaging. Sometimes, a small aneurysm may not be visible due to overlapping with normal branches of the circle of Willis. Analyzing vessels individually, aided by volume rendering techniques, can be helpful in detecting such aneurysms. Additionally, there is the possibility of a "blister" type of aneurysm [8], which represents a local intracranial dissection without a distinct sac. In such cases, irregularities in the arterial wall should be closely examined, particularly near the subarachnoid spaces where the hemorrhage is most significant, as well as in the walls of specific arterial segments.

2. **Intracranial dissection**: Another possibility is a dissecting intracranial arterial abnormality, especially in the V4 segment of the vertebral arteries. Intracranial dissections, particularly those affecting the posterior circulation, can lead to subarachnoid hemorrhage and account for 5% of SAH cases. These dissections are characterized by thinner arterial walls and a lack of an external elastic limiting layer, making them prone to rupture and causing SAH. Detecting intracranial dissections is crucial, as they require specific treatment.
3. **No arterial lesion**: Perimesencephalic hemorrhages (Fig. 5.5), accounting for 5–10% of nontraumatic subarachnoid hemorrhages (SAH) [9], result from venous bleeding that leads to subarachnoid hemorrhage situated in the interpeduncular and peripontine cisterns. The bleeding, while it may extend slightly, remains confined primarily to the suprasellar cisterns and the basal regions of the motor cortex or interhemispheric sulci. Occasionally, a subtle blood presence can be observed in the occipital horns without actual intraventricular hemorrhage. Patients typically present with stable clinical conditions and unimpaired consciousness. Diagnosing perimesencephalic hemorrhage relies on the clinical and radiological criteria mentioned earlier, coupled with the absence of an aneurysmal structure evident in CT angiography or MRA or on the cerebral arteriography of the circle of Willis. The initial clinical manifestations, as well as the long-term outcomes and prognosis, are considerably more favorable compared to SAH caused by aneurysms. Most medical teams opt for a secondary non-invasive investigation into the underlying cause, typically conducted a few weeks after the initial event.

Key Points # 1

- Eighty-five percent of spontaneous SAH arises from aneurysm rupture, usually in the region of the circle of Willis.
- Imaging features associated with aneurysm rupture are size larger than 6 mm, irregular configuration, and smooth concentric aneurysm wall enhancement.
- Perimesencephalic hemorrhage arises from venous bleeding and has a good prognosis.
- Cerebral convexity SAH may result from RCVS or dural AVF.

5.3 Intraparenchymal Hemorrhage

5.3.1 Overview

Intraparenchymal hemorrhage accounts for approximately 15% of all strokes [10]. In older adults, the most common etiologies are hypertension, cerebral amyloid angiopathy, anticoagulation, hemorrhagic transformation of acute ischemic strokes, and underlying primary or secondary tumors. In younger adults and children, common vascular malformations such as arteriovenous malformations, cavernous malformations, and cerebral venous sinus thrombosis and rarer lesions such as moyamoya and dural arteriovenous fistulas

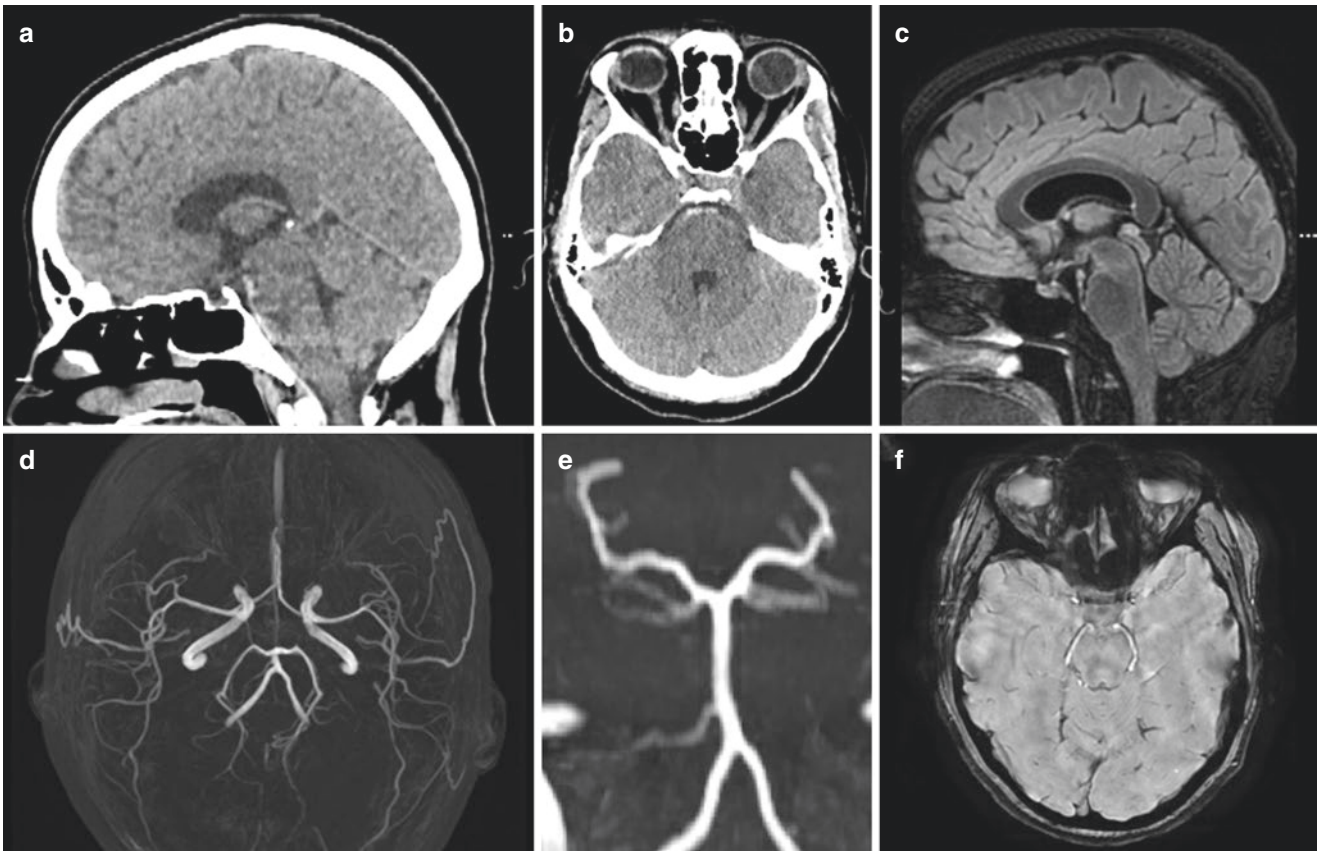

Fig. 5.5 Perimesencephalic hemorrhage is observed on noncontrast CT anterior to the pons (**a**, **b**) and on the FLAIR image (**c**), with no arterial abnormalities detected on angioMR time-of-flight (**d**, **e**) and no lesions detected on susceptibility-weighted imaging (SWI, **f**)

should be considered. Additional rarer causes of IPH include Reversible Cerebral Vasoconstrictive Syndrome (RCVS), posterior reversible encephalopathy syndrome (PRES), vasculitis, drug toxicity, and infections such as mucormycosis and aspergillosis.

5.3.2 Key Imaging Features of Intraparenchymal Hemorrhage

Acute intraparenchymal hemorrhage typically demonstrates homogeneous hyperdensity due to high protein content on NCCT, measuring approximately 40–80 HU. The presence of fluid fluid levels or foci of hypoattenuation (the swirl sign) may represent hyperacute (unclotted) hemorrhage, a coagulation disorder, and/or active bleeding. As the IPH breaks down, it usually becomes isodense to brain at 1–2 weeks and hypodense approaching the attenuation of cerebrospinal fluid at 1–2 months. On MRI in the first few hours, an intracerebral hematoma consists of intact red blood cells containing mainly oxyhemoglobin that is isointense on T1 and hyperintense on T2-weighted images. Over time changes begin at the periphery and extend inward. From 1 to 3 days, the hemorrhage is characterized predominantly by deoxyhemoglobin which is isointense on T1 and hypointense on T2WI. In the early subacute phase (3–7 days), deoxyhemoglobin converts to intracellular methemoglobin which is hyperintense on T1 and hypointense on T2WI. Subsequently at 1–4 weeks, the red blood cells lyse. The extracellular methemoglobin is hyperintense on both T1 and T2WI. After 4 weeks, the resultant cavity shrinks to become slit like and contains mainly hemosiderin laden macrophages with hypointensity on T1 and T2WI (Table 5.1). Oxyhemoglobin and extracellular methemoglobin do not exhibit susceptibility effects, while deoxyhemoglobin, intracellular methemoglobin, and hemosiderin do exhibit susceptibility effects. After the first few hours, since hematomas contain a combination of blood products, they nearly always show blooming on SWI images. Surrounding edema increases for the first 2 weeks and resolves by approximately 1 month. From 1 week to 1 month, following the injection of intravenous gadolinium, there is a smooth rim of enhancement due to an inflammatory response and breakdown of the blood brain barrier.

Key Points # 2

- The timing of IPH can be determined by its CT and MR appearance.
- Imaging features of IPH (swirl sign, intraventricular extension, contrast extravasation, volume, and infratentorial location) can be used to predict hematoma expansion and determine prognosis.

5.3.3 Prognostic Factors

A number of factors should be included when describing hematomas because they predict higher mortality and may require neurosurgical intervention. These include findings that predict hematoma expansion such as areas of hypodensity within a hematoma on noncontrast CT, irregular margin or shape, contrast extravasation on CTA, intraventricular extension, and hematoma size which can be measured using the ABC/2 formula. Brain herniation suggesting the need for hemicraniectomy, and hydrocephalus suggesting the need for shunt placement are also important. Age and Glasgow coma score are key clinical factors that predict mortality. The ICH score incorporates many of these factors and allows an early rapid estimation of patient prognosis [11]. A score of 4 or higher predicts a 97% mortality rate.

5.3.4 Entities with Underlying Vascular Abnormality on CTA or MRA

When a patient presents to the emergency room with a lobar hemorrhage, they typically undergo CT angiography scanning (Table 5.2). Approximately 15% have an underlying large or medium vessel vascular abnormality visualized on CTA. The most common underlying vascular abnormalities in one large study were arteriovenous malformation (43%), aneurysm (24%), and venous sinus thrombosis (19%). Rarer causes include moyamoya syndrome, vasculitis, and reversible cerebral vasoconstriction syndrome [12].

Table 5.1 CT and MR characteristics of intracranial hemorrhage

Time	NCCT	CECT	T1	T2	T2*
Hyperacute (<6 h)	Hyperdense		Isointense	Hyperintense	
Acute (6 h – 3 days)	Hyperdense		Isointense	Hypointense	Hypointense
Early subacute (3–7 days)	Hyper/isodense		Hyperintense rim Isointense center	Hypointense	Hypointense center
Late subacute (1–4 weeks)	Iso/hypodense	Rim enhancement	Hyperintense	Hyperintense	Hypointense
Chronic (months – years)	Hypodense		Hypointense	Hypointense	Hypointense

Density/Intensity compared to normal brain parenchyma. *NCCT* noncontrast CT, *CECT* contrast enhanced CT

Table 5.2 Most common etiologies of intraparenchymal hemorrhage with or without underlying vascular abnormality on CTA

Entity	Clinical	Key imaging features in addition to parenchymal hematoma
Underlying vascular abnormality on CTA		
Arteriovenous malformation	• Age—Children, young adults • Risk factors—Older age, larger size, deep venous drainage, venous stenosis, feeding artery, or intranidal aneurysm • Syndromes—HHT, Wyburn-Mason, RASA • Symptoms—Seizure, headache, acute neurologic deficit • Etiology—Congenital	• Hemorrhage location—Lobar or deep gray nuclei • NCCT—Hyperdense vessels, Ca+ • CTA/MRA—Arterial phase opacification of feeding arteries, nidus, draining veins • T2WI—Flow voids, pulsation artifact • FLAIR—Gliosis, edema
Cerebral venous sinus thrombosis	• Age—Children, young and older adults • Risk factors—Prothrombosis, pregnancy, oral contraceptives, dehydration, infections • Symptoms—Headache, seizure, encephalopathy, acute neurologic deficit • Etiology—Hypercoagulability	• Hemorrhage location—Lobar (superior sagittal, transverse, sigmoid sinus) or deep gray nuclei (ICV, VOG, straight sinus) • NCCT—Hyperdense vein (cord sign), hyperdense sinus (triangle sign) • T2 WI—Absence of flow void • FLAIR—Edema • DWI—Facilitated or restricted diffusion • SWI—Blooming in clotted vessel/vein • CTV, CE MRV, CE MPRAGE, and T2 SPACE all highly sensitive and specific for thrombosis detection
Hemorrhagic transformation of ischemic stroke	• Age—Older adults > young adults and children • Risk factors—Reperfusion therapy, larger stroke size, older age, hypertension, hyperglycemia • Timing—1–4 days • Etiology—Reperfusion into ischemic tissue	• Hemorrhage location—Peripheral petechial > parenchymal (in basal ganglia with MCA M1 strokes) • CTA—Recanalization or persistent clot when reperfusion from collaterals causes hemorrhage • SWI is superior to NCCT for hemorrhage detection
Aneurysm	• Age—Young > older adults • Risk factors—Aneurysm size >5 mm, lobulation, growth between scans • Symptoms—Severe headache, focal neurologic deficit • Etiology—Congenital	• Hemorrhage location—Basal ganglia (M1 segment aneurysm), anterior temporal lobe (MCA bifurcation aneurysm), inferior frontal lobe (anterior communicating artery aneurysm), other (mycotic aneurysms); usually has associated subarachnoid hemorrhage • NCCT—Aneurysm is less hyperdense than clot • T2 WI—Flow void with lamellated appearance • CTA and CE MRA—>90% sensitive and specific for aneurysm detection
Moyamoya	• Age—Children and young adults • Symptoms—Acute neurologic deficits • Associations—Radiation, NF1, Down's syndrome, atherosclerosis • Etiology—Idiopathic	• Hemorrhage location—Basal ganglia • FLAIR—"ivy sign" – Sulcal hyperintensity from slow blood flow in collateral vessels • T2 W1—Flow voids in collateral network and absence of flow voids in distal ICAs and proximal • Strokes of variable ages in anterior circulation and border zone distributions • CTA/MRA—Severe narrowing or occlusion of distal ICAs, proximal MCAs and ACAs with circle of Willis and pial collaterals from posterior circulation • MCAs and ACAs
Reversible cerebral vasoconstriction syndrome	• Age—Young to middle age females • Risk factors—Pregnancy, migraines, vasoactive drugs • Symptoms—Recurrent thunderclap headaches, focal neurologic deficit • Etiology—Reversible vasospasm	• Hemorrhage location—Lobar parenchymal plus cerebral convexity subarachnoid hemorrhage • CTA/MRA—Multifocal stenoses in first and second order branches • DWI—Border zone infarctions • FLAIR—Cortical and subcortical vasogenic edema • Vessel wall imaging—Uniformly thickened walls without enhancement
Primary CNS vasculitis	• Age—Middle age males • Symptoms—Headache, encephalopathy, stroke, seizure • Etiology—T-cell mediated inflammation	• Hemorrhage location—Lobar plus subarachnoid at the cerebral convexities • CTA/MRA—Proximal and/or distal circle of Willis vessel stenoses • DWI/FLAIR—Strokes of different ages in different vascular distributions • CE T1—Leptomeningeal enhancement • Vessel wall imaging—Concentric enhancement

Table 5.2 (continued)

Entity	Clinical	Key imaging features in addition to parenchymal hematoma
Dural AV fistula	• Age—Middle age to older adult • Risk factors—Prior sinus thrombosis, cortical venous drainage • Symptoms—Pulsatile tinnitus, cranial nerve palsies, orbital symptoms, strokes • Etiology—Idiopathic or resulting from trauma, surgery, VST, tumor, infection	• Hemorrhage location—Lobar - cerebellum, medial temporal and occipital lobes; subarachnoid at the cerebral convexities • Time resolved CTA/MRA—Enlarged feeding arteries (ICA, ECA, MMA), direct connection(s) to enlarged draining veins or abnormal venous sinuses with channels and arterialized flow • T2 WI—Abnormal flow voids
Posterior reversible encephalopathy syndrome	• Age—Young adults • Symptoms—Headache, seizure, encephalopathy, visual changes • Etiology—Loss of autoregulation due to acute blood pressure change, neurotoxins	• Hemorrhage location—Lobar hemorrhages in 20% • FLAIR—Edema/ischemia in parietal and occipital subcortical white matter or in border zone distribution • CTA/MRA—Posterior circulation vasoconstriction and/or vasodilatation with beading
Infections	• Age—Any age • Risk factors—Immunocompromised • Etiology—*Mucormycosis/aspergillosis*—Spread from sinonasal cavity to the skull base and circle of Willis *bacterial endocarditis*—Hematogenous spread to distal MCA, ACA, PCA branches	• *Mucormycosis/aspergillosis*—Circle of Willis vascular narrowing and/or pseudoaneurysm formation with basal ganglia hemorrhages, infarctions, abscesses, and edema • *Bacterial endocarditis*—Distal pseudoaneurysms with lobar hemorrhages, abscesses, infarctions, edema
No underlying vascular abnormality on CTA		
Cerebral amyloid angiopathy	• Age—Over 65 • Symptoms—Cognitive impairment, focal neurologic deficits, seizures • Etiology—Deposition of cerebral amyloid- β peptide in walls of small leptomeningeal and cortical vessels	• Hemorrhage location—Lobar • Microhemorrhages at gray–white matter junctions • Leptomeningeal hemorrhage/hemosiderosis • Periventricular leukoencephalopathy • Cortical/subcortical lacunes • Prominent perivascular spaces • Leptomeningeal enhancement (inflammatory CAA) • Vasogenic edema (inflammatory CAA)
Hypertensive vasculopathy	• Age—Older adults • Symptoms—Acute neurologic deficits • Etiology—Poorly controlled hypertension	• Hemorrhage location—Basal ganglia, thalami, brainstem, cerebellum • Microhemorrhages • Lacunar infarctions • Diffuse leukoaraiosis
Cavernous malformation	• Age—40–60 • Risk factors—Radiation • Symptoms—Acute neurologic deficits, seizures • Etiology—Hyalinized thin-walled capillaries with surrounding hemosiderin	• Central "popcorn" appearance with T1 hyperintense foci • Complete hemosiderin rim • Enhancement due to central leakage of contrast • Edema if recent bleeding • Numerous additional lesions seen only on SWI in familial forms
Tumoral hemorrhage	• Age—Older adults • Risk factors—Chemotherapy, radiation, hypertension, anticoagulation • Symptoms—Acute neurologic deficits, seizures • Etiology—Rupture of tumoral blood vessels, tumoral invasion of parenchymal arteries or veins	• Enhancing tissue • Delayed evolution of products of hemorrhage • Incomplete hemosiderin rim • Fluid fluid levels or blood cystic-necrotic levels • Disproportionately large amount of edema
Hemorrhagic encephalitis	• Age—Any age • Symptoms—Fever, encephalopathy, seizures • Etiology—Herpes virus, flaviviruses, Epstein–Barr virus	• FLAIR/T2 hyperintense expansile lesions with hemorrhage involving cortex and subcortical white matter • Herpes simplex virus—Limbic system • Flaviviruses, Epstein–Barr virus—Basal ganglia, thalami, brainstem

5.3.4.1 Arteriovenous Malformation

An arteriovenous malformation is composed of large feeding arteries, a central nidus through which arteriovenous shunting occurs and enlarged draining veins. AVMs are most commonly intraparenchymal but may be intraventricular or located in the subarachnoid space [13]. Eighty-five percent of AVMs are supratentorial, and approximately 65% of supratentorial AVMs are superficial (lobar). They are typically sporadic but may be associated with syndromes such as hereditary hemorrhagic telangiectasia, Wyburn-Mason syndrome, or the RASA 1 mutation. AVMs are typically diagnosed in childhood or young adulthood. Risk of rupture

increases with age, presence of a feeding artery or intranidal aneurysm, venous stenosis, or deep venous drainage.

AVMs are typically classified according to the Spetzler Martin grading system in order to predict the risk of surgical complication based on size, presence of deep venous drainage, and eloquence of location. The hemorrhagic risk is higher for AVMs that are infratentorial, have a deep location and/or deep venous drainage, or have previously bled. AVMs may have calcifications and appear mildly hyperdense on noncontrast CT, enhance during the arterial phase on CTA and dynamic contrast-enhanced MRA, and have prominent flow voids and pulsation artifact on T2-weighted MRI images. Additional features may include edema or gliosis (best identified on FLAIR images) and acute or chronic hemorrhage (best identified on SWI images) in the surrounding brain parenchyma. Digital subtraction angiography remains the gold standard for diagnosing and assessing AVMs.

5.3.4.2 Cerebral Venous Sinus Thrombosis

Cerebral venous sinus thrombosis refers to the formation and propagation of clot leading to occlusion of intracranial venous sinuses and veins. Important risk factors are prothrombotic conditions, pregnancy, oral contraceptives, dehydration, infectious and inflammatory conditions, and malignancy. Symptoms and imaging findings vary by location [14]. The most common symptoms are headache, seizure, encephalopathy, and focal neurologic deficits. Lobar hemorrhages are typically caused by thrombosis of the superior sagittal, transverse and sigmoid sinuses, and/or of cortical veins (Fig. 5.6). Basal ganglia and thalamic hemorrhages

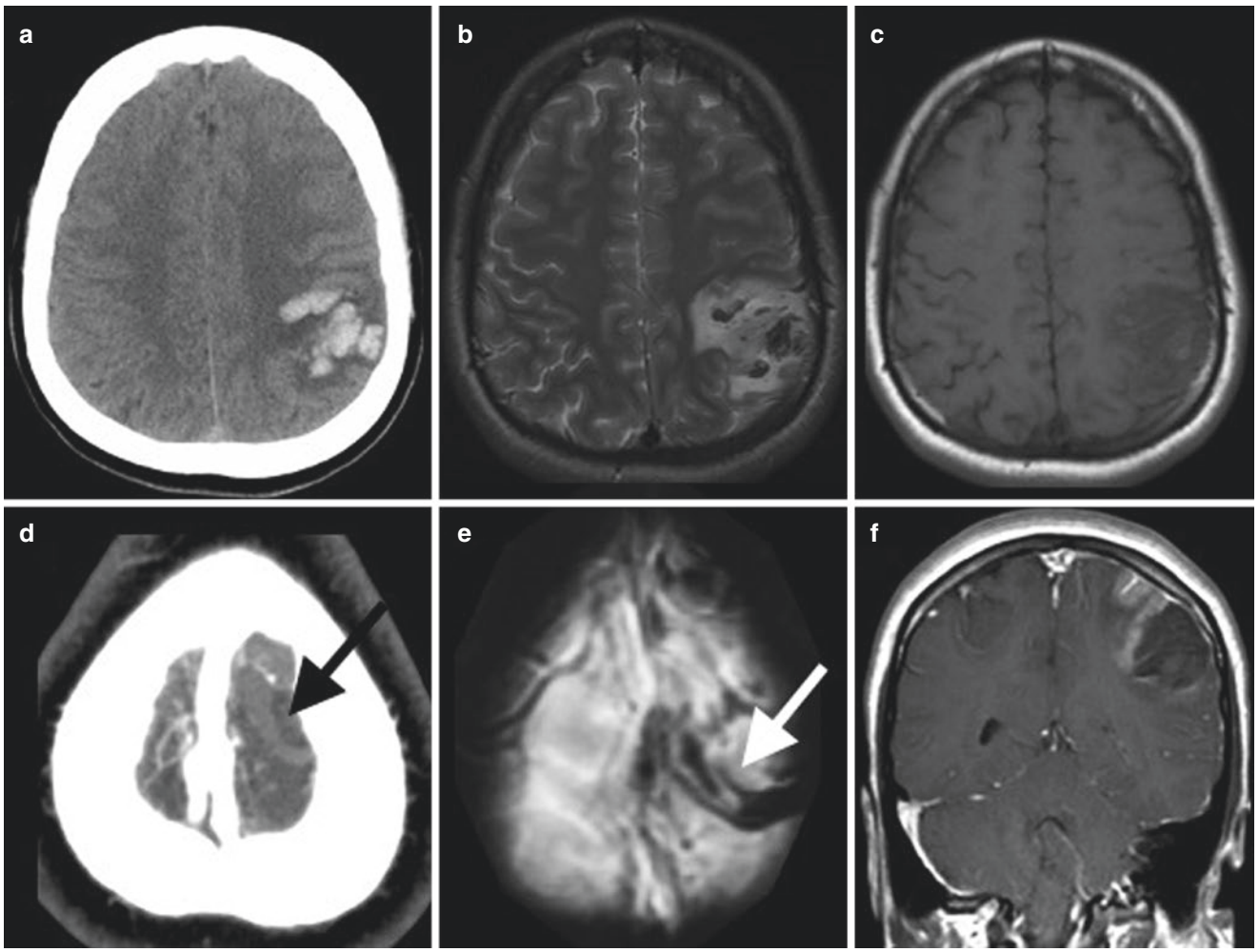

Fig. 5.6 A 36-year-old female with severe headache, right-sided weakness, and cortical vein thrombosis. Noncontrast CT (**a**) shows a left parietal parenchymal hematoma. The hematoma has areas that are hypointense on T2-weighted images (**b**) and isointense on T1-weighted images (**c**), consistent with deoxyhemoglobin and areas that are hyperintense on T2-weighted images and isointense on T1-weighted images, consistent with oxyhemoglobin. CTA source images (**d**) show nonopacification of a cortical vein, consistent with thrombosis (black arrow). There is blooming of the vein on the gradient echo images (**e**), confirming thrombosis. Coronal contrast-enhanced T1-weighted images (**f**) show gyriform enhancement, typical of subacute ischemic lesions

are typically caused by thrombosis of the internal cerebral veins, vein of Galen, or straight sinus. Findings on NCCT include hyperdensity in the thrombosed vein (cord sign) or sinus (dense triangle sign), present in approximately 30% of cases, as well as parenchymal hemorrhage in a nonarterial distribution and/or vasogenic edema and mass effect. CT venography is over 90% sensitive and specific for the detection of CVT. Findings on MRI include absence of a normal flow void on T2 weighted images. The clot and parenchymal hematoma are typically characterized by T1 isointensity and T2 hypointensity in the acute stage, by T1 hyperintensity and T2 hypointensity in early subacute stage and by T1 and T2 hyperintensity in the late subacute stage. Edema is typically best visualized on the FLAIR images and is characterized by restricted and/or facilitated diffusion. Contrast-enhanced MR venography, contrast-enhanced volumetric T1-weighted images, and T2 volumetric SPACE sequences demonstrate higher than 90% sensitivity and specificity for detection of CVT.

5.3.4.3 Hemorrhagic Transformation of Ischemic Stroke

Hemorrhagic transformation of acute ischemic stroke has been variably reported. Risk factors include reperfusion therapy with intravenous thrombolytic agents and/or thrombectomy, larger stroke size, older age, hypertension, and hyperglycemia [15]. Most hemorrhagic transformation manifests as petechial hemorrhage with small isodense or hyperdense peripheral foci on CT that bloom on SWI and is asymptomatic. A minority results in parenchymal hematoma which is typically in the basal ganglia in large anterior circulation strokes. In patients who receive IVtPA, hemorrhagic transformation typically occurs in the first 24 h and is symptomatic in 6%. Spontaneous hemorrhage occurs up to 4 days after stroke onset and is symptomatic in 3%. Following reperfusion therapy, dual-energy CT can be used to distinguish between contrast blush and hemorrhage.

5.3.4.4 Aneurysm

Aneurysms typically present with subarachnoid hemorrhage but can present with isolated IPH when they are located at the M1 segment and point superiorly into the basal ganglia, at the MCA bifurcation and point posteriorly into the temporal lobe, or at the anterior communicating artery and point superolaterally into the inferior frontal lobe. Peripheral mycotic aneurysms can also rupture into adjacent brain parenchyma (Fig. 5.7). Proximal aneurysms that cause isolated IPH are typically greater than 12 mm [16]. On NCCT, they are less hyperdense than the adjacent hematoma, but may have a partially thrombosed hyperdense wall similar in density to the adjacent hematoma. On MRI, aneurysms show a flow void on T2WI with a lamellated appearance with signal intensity depending on the stage of hemorrhage if there is partial thrombosis. Aneurysms may be associated with pulsation artifact. CTA and contrast-enhanced MRA are greater than 90% sensitive and specific for identifying aneurysms.

5.3.4.5 Moyamoya Syndrome

Moyamoya disease is an idiopathic, non-arteriosclerotic, noninflammatory arterio-occlusive syndrome that occurs in young children and young adults. It is characterized predominantly by progressive occlusion of the distal internal carotid arteries and of the proximal anterior and middle cerebral arteries, although the posterior circulation can be involved in up to 50% [17]. As a compensatory mechanism, multiple collateral vessels form in the region of the circle of Willis and involve the lenticulostriate and thalamoperforating arteries as well as leptomeningeal and dural arteries. Pial collaterals, typically from the posterior circulation, also form. Children typically present with borderzone and subcortical white matter infarctions, while young adults more commonly present with basal ganglia hemorrhage due to rupture of collateral vessels (Fig. 5.7). CTA and MRA are highly sensitive for identifying the large vessel occlusions and stenoses and larger collateral vessels, but digital angiography remains the gold standard for delineating the extent of collateral vessels. Findings on MRI include abnormal flow voids on T2 WI, the ivy sign (sulcal FLAIR hyperintensity due to slow flow in collateral vessels), acute ischemic strokes, and intraparenchymal hemorrhage including microhemorrhages in the basal ganglia and deep white matter. Moyamoya syndrome refers to a number of conditions that mimic MMD on imaging. These include atherosclerosis, hematologic disorders such as sickle cell disease, inflammatory and infectious etiologies, and radiation therapy. Treatment includes surgical direct revascularization options such as MCA to STA bypass or indirect revascularization options such as EDAS (encephaloduroarteriosynangiosis).

5.3.4.6 Reversible Cerebral Vasoconstriction Syndrome

Reversible cerebral vasoconstriction syndrome is characterized by rapid onset of frequently recurrent thunderclap headaches and cerebral vasospasm that resolves by 12 weeks. The syndrome occurs most frequently in young to middle age adult females and is associated with pregnancy, migraines, and the use of vasoactive drugs such as triptans, amphetamines, selective serotonin reuptake inhibitors, and cocaine. CTA, MRA, and DSA show smooth, tapered narrowing of large- to medium-sized arteries (first- and second-order branches) followed by abnormally dilated segments or a beaded appearance distal to the stenoses (Fig. 5.7). Lobar hemorrhages occur in up to 20%, subarachnoid hemorrhage at the cerebral convexity in up to 35%, border zone infarctions in nearly 30%, and cortical and subcortical vasogenic edema in nearly 40% [18]. Of note, FLAIR identifies the extent of edema, DWI readily dif-

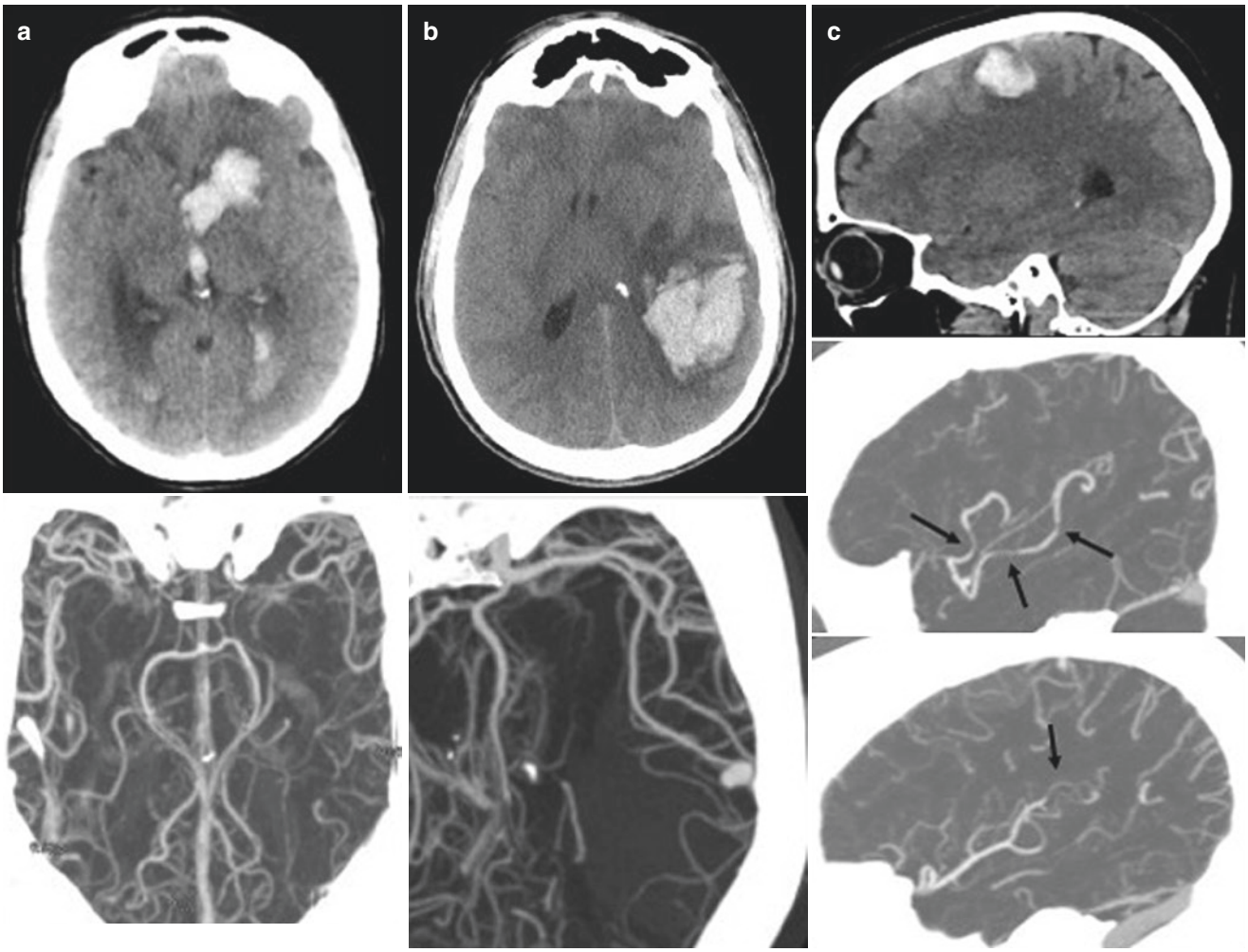

Fig. 5.7 Multiple entities with parenchymal hematomas and underlying vascular lesion on CTA or MRA Patient 1 with moyamoya, Column **a**—The top image shows left caudate head hemorrhage with extension into the lateral and third ventricles. The lower image shows severe attenuation of the bilateral M1 and A1 segments with collateral vessels. Patient 2 IV drug abuser with mycotic pseudoaneurysm, Column **b**—The top image shows a left temporal parenchymal hematoma. The lower image shows an underlying distal MCA mycotic pseudoaneurysm. Patient 3 with reversible cerebral vasoconstrictive syndrome, Column **c**—The top image shows right posterior frontal intraparenchymal and subarachnoid hemorrhage. The middle and lower images show stenoses (arrows) in bilateral MCA branches

ferentiates between vasogenic and cytotoxic edema, FLAIR sulcal hyperintensity can reflect subarachnoid hemorrhage or slow flow in collateral vessels and SWI can delineate the extent of hemorrhage. Vessel wall imaging typically shows uniformly thickened wall that does not enhance. Treatment includes calcium channel blockers and 90% of patients recover without persistent neurologic deficits.

5.3.4.7 Miscellaneous

Infections

Intracranial infections can lead to intraparenchymal hemorrhage due to arterial invasion with mycotic aneurysm formation and rupture. Mucormycosis and aspergillosis are angioinvasive fungal infections that occur in the sinonasal cavity. They can directly invade the skull base with spread to the circle of Willis leading to basilar meningitis, pseudoaneurysm formation, basal ganglia hemorrhages, infarctions, and abscesses. Bacterial organisms associated with infectious endocarditis can spread hematogenously to gray–white matter junctions where infection leads to peripheral pseudoaneurysm formation, lobar hemorrhages, infarctions, and abscesses. While varicella vasculopathy is typically associated with vascular narrowing and ischemic infarctions, aneurysms can form and result in intraparenchymal or subarachnoid hemorrhage.

Primary CNS Vasculitis

Primary CNS vasculitis occurs most frequently in middle age males and is thought to result from T-cell mediated inflammation of medium and small brain parenchymal and leptomeningeal arteries. Common presenting symptoms are headache, encephalopathy, strokes, and seizures. Common imaging findings include proximal and/or distal stenoses in 60%, parenchymal hemorrhages and hemorrhagic infarctions, strokes of different ages in different vascular distributions, leptomeningeal enhancement, subarachnoid hemorrhage at the cerebral convexities, and concentric vessel wall enhancement [19]. Treatment is with steroids and cytotoxic agents. Systemic vasculitides can have similar CNS findings but are distinguished by their involvement of multiple organ systems.

Dural AV Fistula

Dural arteriovenous fistulas (dAVFs) are acquired vascular malformations in which there are abnormal connections between arteries that typically supply the meninges and the dural venous sinuses. Symptoms depend on the fistula location and whether or not there is brain edema or hemorrhage and include pulsatile tinnitus, cranial nerve palsies, orbital symptoms (cavernous carotid fistulas), and focal neurologic deficits. In one large study, approximately 24% of patients had intracranial hemorrhage with 52% having isolated intraparenchymal hemorrhage, 22% having isolated SAH, and 23% having both [20]. The fistula involved the tentorium, petrosal sinuses, torcular, transverse sinuses, and/or foramen magnum in 66%. The IPH was usually located near the point of fistulization in the cerebellum or medial temporal or occipital lobes. The risk of hemorrhage is higher when there is cortical venous drainage, and nearly all patients with dural AVF and intracranial hemorrhage have cortical venous reflux. Time-resolved CTA and MRA are over 90% sensitive for detecting dural AVF [21]. CTA and MRA findings include enlarged internal carotid, external carotid or meningeal arteries, enlarged transosseous vessels, an abnormal dural venous sinus (abnormal channels, early filling, and arterialized flow), and dilated cortical and meningeal veins. These abnormal vessels can also be visualized as abnormal flow voids on T2WI. SWI images may show intraparenchymal, subarachnoid, intraventricular, or subdural hemorrhage. Brain parenchymal edema (best seen on FLAIR images) may also be present. The Cognard and Borden scales address the type of venous drainage which predict the future risk of hemorrhage.

Pres

Posterior Reversible Encephalopathy Syndrome is a neurotoxic state characterized by loss of autoregulation and disruption of the blood–brain barrier due to acute changes in blood pressure and/or circulating toxins. Typical presenting symptoms are headache, seizures, encephalopathy, and visual changes. Key imaging findings are FLAIR/T2 hyperintense edema in the parietal and occipital subcortical white matter and cortex and/or in a borderzone distribution. Affected regions can have parenchymal hemorrhages in up to 15% and infarctions characterized by restricted diffusion in 10–25% [22]. CTA, MRA, and DSA can show foci of vasoconstriction, vasodilation, or both (a beaded appearance).

5.3.5 Entities with No Underlying Vascular Abnormality on CTA or MRA

When a patient presents to the emergency room with a lobar hemorrhage, they typically undergo CT angiography scanning. In approximately 85%, the CTA or MRA does not demonstrate a causative vascular lesion. The most common intraparenchymal hemorrhages in this situation result from hypertension, cerebral amyloid angiopathy, coagulopathy, or underlying tumor.

5.3.5.1 Cerebral Amyloid Angiopathy

Cerebral amyloid angiopathy is a cerebrovascular disease that results from deposition of cerebral amyloid-β peptide in the walls of small leptomeningeal and cortical vessels. CAA is the cause of up to 50% of spontaneous intracerebral hemorrhages in patients older than 65 years of age, and the incidence increases with age. For example, approximately 5–9% of people between ages 60 and 69 have amyloid deposition at autopsy while 43–58% of people over 90 years of age have amyloid deposition at autopsy [23]. Common presentations are headache, focal neurologic deficits, seizures, and cognitive impairment. The Boston criteria 2.0 (Table 5.3) combine clinical, radiographical, and pathological criteria to determine the probability of diagnosis [24]. Key imaging features are lobar hemorrhage, microhemorrhages at gray–white matter junctions, leptomeningeal hemorrhage and hemosiderosis, periventricular leukoencephalopathy, cortical/subcortical lacunes, and prominent perivascular spaces (Fig. 5.8). Inflammatory CAA has additional findings of leptomeningeal enhancement and vasogenic edema and tends to present at a

Table 5.3 Boston Criteria 2.0 for sporadic cerebral amyloid angiopathy

1. Definite CAA	Full post-mortem examination demonstrating: • Presentation with spontaneous ICH, TFNEs, cSAH, or CI/dementia • Severe CAA with vasculopathy • Absence of other diagnostic lesion
2. Probable CAA with supporting pathology	Clinical data and pathologic tissue (evacuated hematoma or cortical biopsy) demonstrating: • Presentation with spontaneous ICH, TFNEs, cSAH, or CI/dementia • Some degree of CAA in specimen • Absence of other diagnostic lesion
3. Probable CAA	Clinical data and MRI demonstrating • Age ≥ 50 years • Presentation with spontaneous ICH, TFNEs, or CI/dementia • ≥2 of the following strictly lobar hemorrhagic lesions on T2* weighted MRI, in any combination – ICH, CMB, cSS/cSAH foci OR • 1 lobar hemorrhagic lesion +1 white matter feature (severe CSO-PVS or WMH-MS) • Absence of any deep hemorrhagic lesions (ICH, CMB) on T2*- weighted MR • Absence of other cause of hemorrhagic lesions • Hemorrhagic lesion in cerebellum not counted in either lobar or deep hemorrhagic lesion
Possible CAA	Clinical data and MRI demonstrating • Age ≥ 50 years • Presentation with spontaneous ICH, TFNEs, or CI/dementia • Absence of other cause of hemorrhage • 1 strictly lobar hemorrhagic lesion on T2* weighted MRI: ICH, CMB, cSS/cSAH focus OR • 1 white matter feature (severe CSO-PVS or WMH-MS) • Absence of any deep hemorrhagic lesions (ICH, CMB) on T2*- weighted MR • Absence of other cause of hemorrhagic lesions • Hemorrhagic lesion in cerebellum not counted in either lobar or deep hemorrhagic lesion

ICH intracranial hemorrhage, *TFNE* transient focal neurologic episode, *cSAH* convexity subarachnoid hemorrhage, *CI* cognitive impairment, *CMB* cerebral microbleed, *cSS* cortical superficial siderosis, *CSO-PVS* visible centrum semiovale perivascular spaces, *WMH-MS* white matter hyperintensities in a multispot pattern

slightly younger age. CAA is most commonly sporadic but numerous rare hereditary types, that are typically autosomal dominant and present in middle age, have also been described.

5.3.5.2 Hypertensive Hemorrhage

Long standing, poorly controlled hypertension is the most common cause of intracranial hemorrhage. Patients develop hypertensive vasculopathy characterized by lipohyalinosis in small- and medium-sized vessels such as the lenticulostriate, thalamoperforating, and pontine perforating arteries as well as cerebellar arterioles. Hemorrhages result from the rupture of microaneurysms with a rebleed rate of 2% per year, and most frequently occur in the basal ganglia (35–40%), thalami (10–20%), pons (5–10%), and cerebellum (5–10%) [25] (Fig. 5.9). Hemorrhages occasionally occur in the subcortical white matter (1–2%). Presenting symptoms vary depending upon the hemorrhage location. Microhemorrhages and lacunar infarctions in the deep gray nuclei, brainstem and cerebellum, and diffuse leukoaraiosis support the diagnosis.

5.3.5.3 Cavernous Malformation

Cavernous malformations are composed of clusters of hyalinized thin-walled capillaries with surrounding hemosiderin. The majority are sporadic and remain asymptomatic. Symptomatic lesions typically present between ages 40 and 60 with headache, seizures, or focal neurologic deficits. Ten to thirty percent are multiple and seen in association with familial multiple cavernous malformation syndrome for which mutations in the KRIT1, CCM2, and PDCD10 genes have been identified. Cavernous malformations can also develop after radiation therapy. On CT, cavernous malformations are usually mildly hyperdense with foci of calcification in 40–60%. On MRI, they have a variable appearance depending on the stage of internal blood products with a central "popcorn appearance," characterized by foci of T1 hyperintensity and isointensity and T2 hyperintensity and hypointensity [26] (Fig. 5.10). They typically have a smooth, complete hemosiderin rim that is hypointense on T2 WI. Lesions show marked blooming on SWI images. In addition, SWI images detect small lesions that are not seen on other MRI sequences. Cavernous malformations may enhance due to leakage of contrast into them and may have surrounding edema if they have recently bled. Cavernous malformations are occasionally associated with developmental venous anomalies.

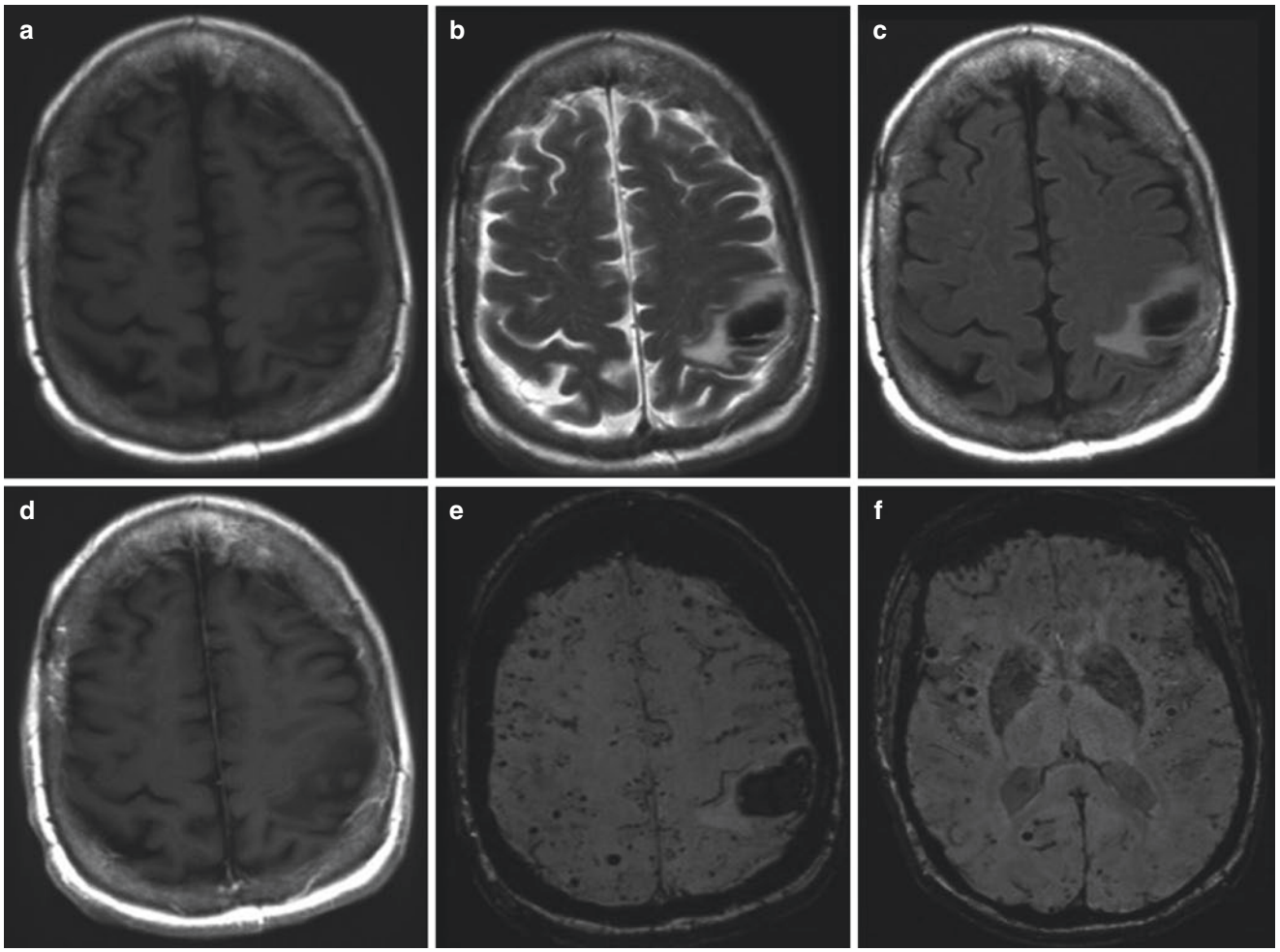

Fig. 5.8 A 70-year-old female with right-sided weakness and amyloid angiopathy. There is an acute parenchymal hematoma in the left parietal lobe that isointense on T1-weighted images (**a**), hypointense on T2 (**b**), and FLAIR (**c**) weighted images, does not show and underlying lesion on gadolinium-enhanced T1-weighted images (**d**) and blooms on SWI (**e**). SWI images (**e** and **f**) show microhemorrhages at gray–white matter junctions as well as hemosiderosis in left frontal sulci

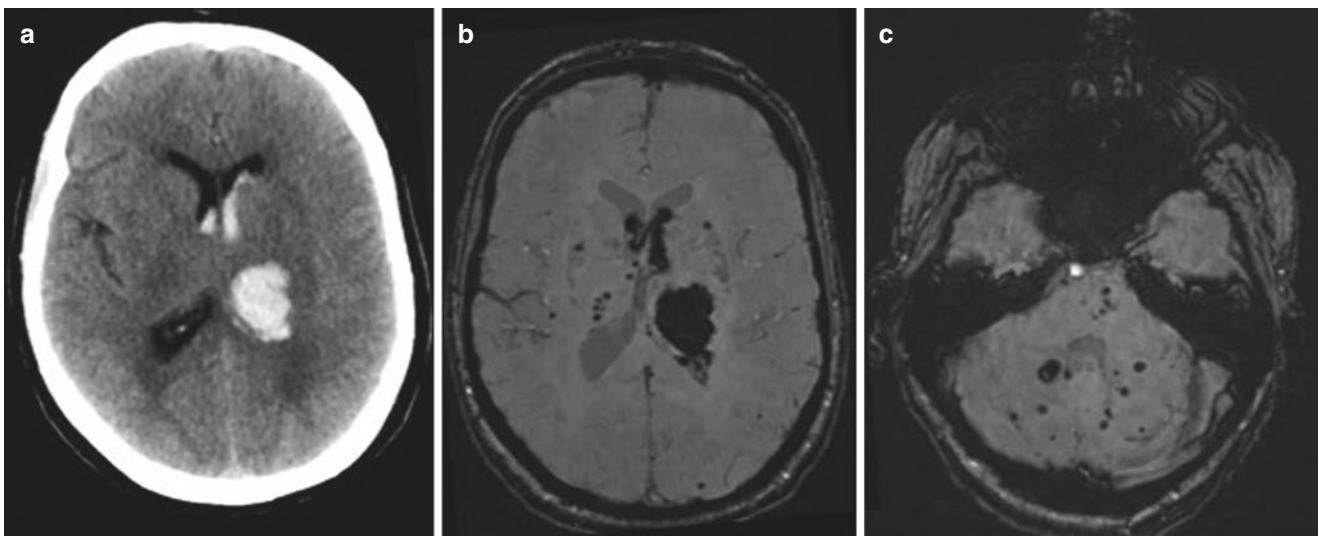

Fig. 5.9 A 53-year-old female with unsteady gait, confusion, and hypertensive hemorrhages. Noncontrast CT (**a**) shows acute hemorrhage in the left thalamus with intraventricular extension. SWI images (**b** and **c**) confirm hemorrhage in the left thalamus and ventricles and show microhemorrhages in the cerebellum, pons, and deep gray nuclei

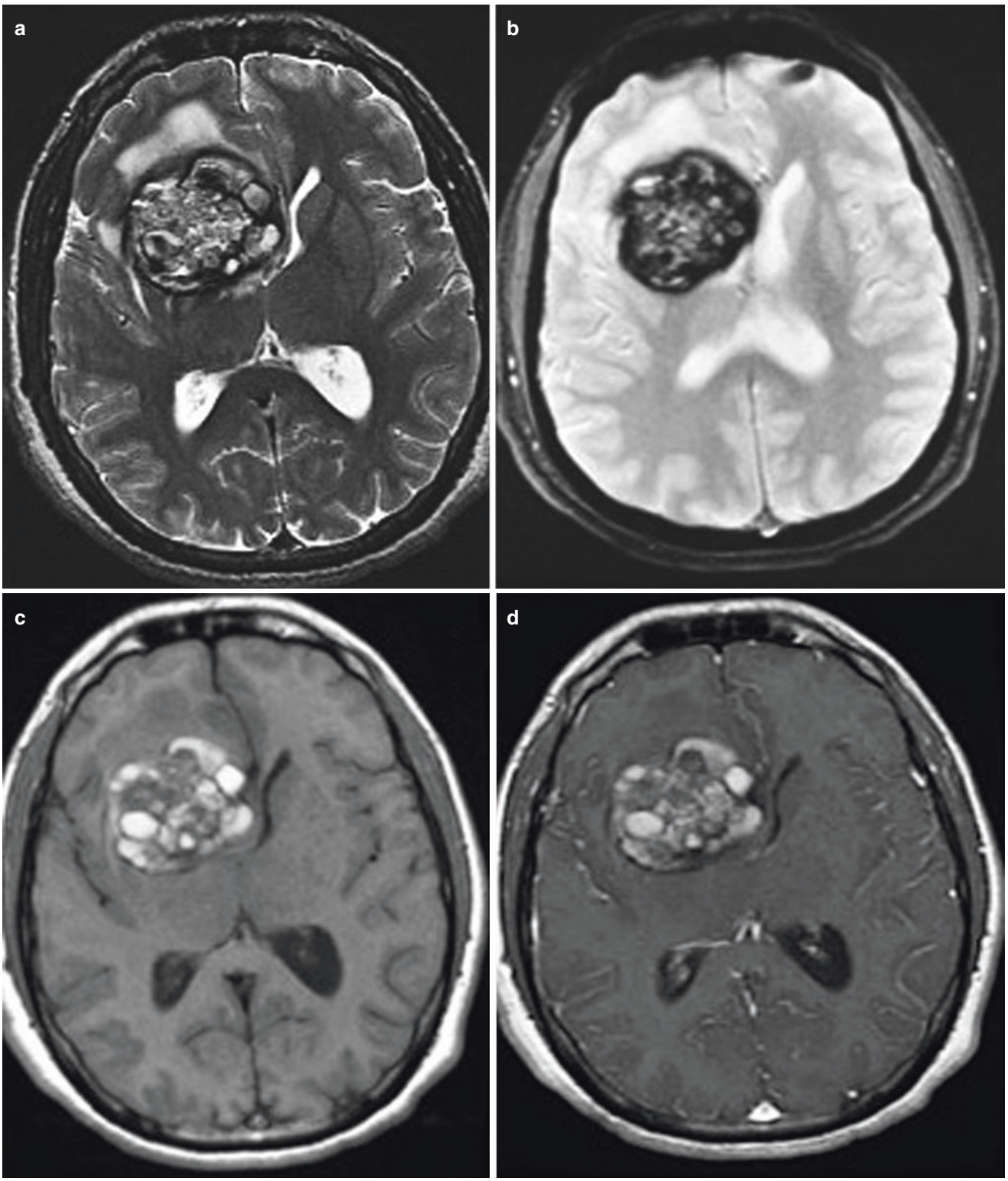

Fig. 5.10 A 50-year-old male with left-sided weakness and a cavernous malformation with a "popcorn" appearance. There is a hemorrhagic mass in the right basal ganglia and right frontal lobe characterized by heterogeneous signal on T2 (**a**) and T1 (**c**) weighted images with foci of T1 hyperintensity consistent with methemoglobin. There is blooming on the GRE images (**b**) due to the subacute and chronic products of hemorrhage. A smooth, complete hemosiderin rim is seen on T2 and GRE (**b**) images. There is no enhancement on gadolinium-enhanced T1-weighted images (**d**)

5.3.5.4 Tumoral Hemorrhage

Approximately 5% of intraparenchymal hemorrhages are secondary to intratumoral or peritumoral hemorrhage. Intratumoral hemorrhage may result from rupture of tumoral blood vessels, tumoral invasion of parenchymal blood vessels, and tumor necrosis. Intratumoral or peritumoral hemorrhage can also result from radiation therapy or chemotherapy. Other risk factors include hypertension, anticoagulation, and advanced age. Tumors most commonly associated with intratumoral hemorrhage are high grade primary tumors such as high grade glial neoplasms, and metastases, most commonly from breast carcinoma, melanoma, renal cell carcinoma, thyroid carcinoma, and choriocarcinoma. Thrombotic tumor emboli from atrial myxoma, thrombotic coagulopathy, and venous sinus thrombosis from tumor invasion or malignancy induced coagulopathy may also result in intraparenchymal hemorrhage in cancer patients. Imaging findings that suggest an underlying tumor include: (1) enhancing tissue, (2) delayed evolution of the products of hemorrhage, (3) an incomplete hemosiderin rim, (4) the presence of multiple foci of susceptibility, (5) the presence of fluid fluid levels or blood-cystic necrotic levels, and (6) the presence of a disproportionately large amount of edema (Fig. 5.11).

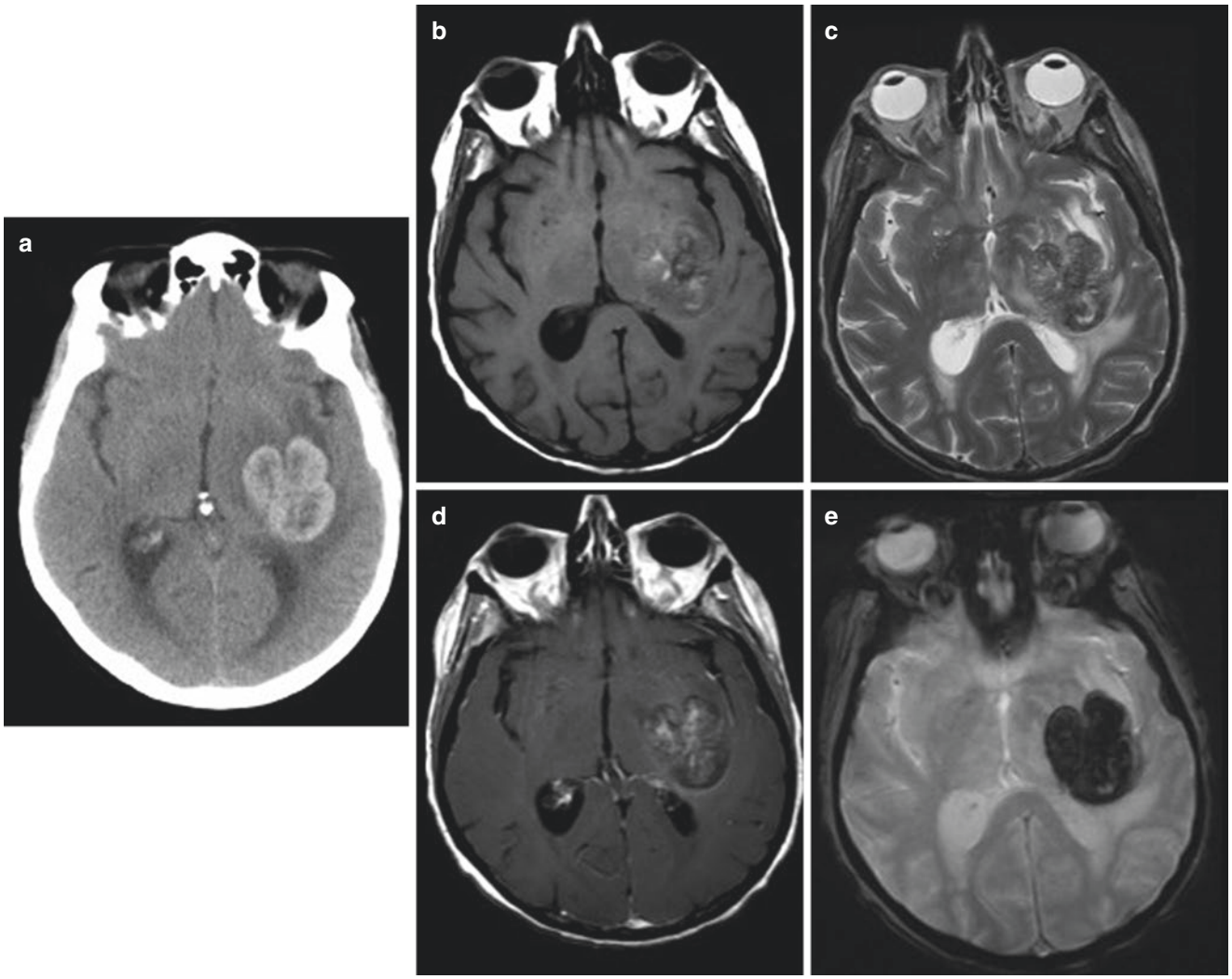

Fig. 5.11 A 65-year-old female with acute right-sided weakness and a hemorrhagic breast carcinoma metastasis. Noncontrast CT (**a**) shows parenchymal hemorrhage in the left basal ganglia and external capsule with surrounding edema. The hemorrhage is heterogenous with hyperintense foci on T1-weighted images (**b**) consistent with methemoglobin and hypointense foci on T2-weighted images, consistent with deoxyhemoglobin or intracellular methemoglobin (**c**). Following the administration of gadolinium (**d**), there is patchy enhancement confirming the presence of an underlying mass. GRE images (**e**) show blooming consistent with hemorrhage

5.3.5.5 Coagulopathy

Approximately, 0.3–0.6 percent of patients on oral anticoagulant therapy have intracranial hemorrhage, most commonly in an intraparenchymal lobar or cerebellar location [27]. Large or multiple synchronous hemorrhages, the presence fluid-fluid levels, and intraventricular extension are characteristic features of both congenital and acquired coagulation disorders. In addition, hemorrhages due to coagulopathy have an increased incidence of ongoing bleeding.

5.3.5.6 Hemorrhagic Encephalitis

Herpes simplex virus is a necrotizing meningoencephalitis that occurs due to latent reactivation in the case of immunosuppression or other stress. It typically involves the limbic system in a bilateral asymmetric distribution. Typical imaging findings include FLAIR/T2 hyperintense edema in the medial temporal lobes, insula, and cingulate gyri with areas of restricted diffusion due to cytotoxic edema, and blooming on SWI due to hemorrhage. Gyriform enhancement is present in the subacute stage. Other viruses that may cause hemorrhagic encephalitis include the flaviviruses (dengue, Japanese, Murray Valley, Powassan, St Louis, Rocio, and West Nile) and Epstein–Barr virus that typically involve the basal ganglia, thalami, and brainstem in varying patterns.

Key Points #3

- Common causes of lobar IPH without underlying vascular abnormality on CTA are amyloid angiopathy, coagulopathy, and underlying tumor and cavernous malformations in younger patients. The presence of microhemorrhages, underlying enhancement or a "popcorn appearance" can help differentiate these entities.
- Deep gray nuclei, brainstem, and cerebellar intraparenchymal hemorrhages without underlying vascular abnormality on CTA are most commonly caused by hypertension. Associated microhemorrhages and lacunar infarcts are common.

Key Points #4

- Common causes of IPH with underlying vascular abnormality on CTA are AVM, cerebral venous sinus thrombosis, and hemorrhagic transformation of acute ischemic stroke.
- AVMs have abnormal flow voids on T2W1 as well as a feeding artery, nidus, and early venous opacification on CTA.
- Cerebral venous sinus thrombosis is characterized by hyperdense vein or sinus on CT, and lack of flow void on T2WI. CTA and MRV are highly accurate for detection.
- Hemorrhagic transformation of ischemic stroke occurs in a vascular territory and is associated with large vessel occlusion.

5.4 Other Hemorrhage

5.4.1 Microhemorrhage

Microhemorrhages are punctate brain hemorrhages which result from rupture of tiny vessels measuring less than 200 μm in diameter and are best seen on SWI images. As mentioned above, they are most commonly seen in a peripheral distribution in association with amyloid angiopathy or concentrated in the deep gray nuclei, brainstem, and cerebellum in association with hypertension. Multiple microhemorrhages are also seen in patients with familial cavernous malformations, CADASIL in 25–70% of cases, history of cardiac bypass surgery, cerebral vasculitis, hemorrhagic micrometastases, fat emboli, septic emboli, and radiation induced cerebral vasculopathy. Microhemorrhages have also been reported in critically ill patients with acute respiratory distress syndrome, high altitude sickness, and Covid 19 who have coagulation impairment and thrombotic microangiopathy.

5.4.2 Subdural and Epidural Hemorrhage

Subdural and epidural hemorrhage are usually associated with head trauma. However, they may occur spontaneously in patients who are receiving anticoagulants or antiplatelet therapy. They can also occur in patients with coagulopathies, dural and osteodural arteriovenous fistulas, intracranial hypotension, and dural or calvarial metastases.

5.5 Blood Mimics

5.5.1 On CT

Distinguishing between acute hemorrhage and hyperattenuating mimics poses a common challenge on CT in neuroradiology. Certain materials with high atomic numbers, such as iodine, calcium, and silicone oil, can exhibit similar attenuation levels to acute blood components, depending on their

concentration. Dual-energy CT offers a solution to differentiate between hemorrhage and these high atomic number materials due to their distinct absorption patterns of X-ray photons at different incident energy levels.

5.5.2 On MR

Fat and blood both appear hyperintense on T1W and T2W FSE sequences. Relying solely on these conventional sequences to distinguish between the two is insufficient. However, fat-suppressed sequences can help determine the correct diagnosis. The Gradient Echo (GRE) and susceptibility-weighted imaging (SWI) sequences, utilizing T2*W-based contrast, are typically employed for the detection of hemorrhage, calcification, and iron accumulation in different tissue types. Since these entities all show low signal on GRE and SWI., differentiating between them can be a genuine challenge. SWI filtered phase images can be useful since hemosiderin and deoxyhemoglobin (both paramagnetic) have signal that is opposite to that of calcium (diamagnetic). Additionally, it is worth noting that two other etiologies, proteinaceous cysts (e.g., colloid cysts) and dense cell packing (lymphoma), can be hyperintense on T1-weighted images and mimic methemoglobin.

5.6 Conclusion

Neuroimaging plays an essential role in management of intracranial hemorrhage. It allows the identification and characterization of intracranial hemorrhage according to location, volume, extent, and age. In conjunction with patient demographics, neuroimaging allows the determination of underlying etiology and is a cornerstone for determining prognosis and appropriate treatment.

Take-Home Messages

- The imaging characteristics of intracranial hemorrhages vary predictably over time for both CT and MRI.
- For SAH, the etiology can be determined by location and findings on CTA. FLAIR is more sensitive than NCCT. The Modified Fisher Grade predicts the risk of vasospasm.
- For IPH without an underlying vascular abnormality on CTA or MRA, amyloid angiopathy (with lobar IPH, peripheral microhemorrhages, and hemosiderosis) and hypertension (with deep gray nuclei, brainstem, or cerebellar IPH and microhemorrhages) are common etiologies.
- For IPH with abnormal vessels on CTA, common etiologies are AVM (with feeding artery, nidus and arterialized vein), cerebral venous sinus thrombosis (with hyperdense vein or sinus that doesn't opacify on CTA), hemorrhagic transformation of ischemic stroke (with large vessel occlusion), dural AVF (with a direct connection between feeding artery and vein), and moyamoya (with severe stenosis of the distal ICAs and proximal ACAs and MCAS) are relatively common etiologies.
- Calcification and other materials with high atomic numbers can mimic hemorrhage on NCCT. Dual energy CT can help differentiate these entities. Calcification, proteinaceous material, melanin, iron, and dense cell packing can mimic hemorrhage on MRI. SWI-filtered phase images can sometimes help differentiate calcification from hemorrhage.

References

1. Claassen J, Park S. Spontaneous subarachnoid haemorrhage. Lancet. 2022;400:846–62.
2. Edjlali M, Rodriguez-Régent C, Hodel J, et al. Subarachnoid hemorrhage in ten questions. Diagn Interv Imaging. 2015;96:657–66.
3. Etminan N, Chang H-S, Hackenberg K, et al. Worldwide incidence of aneurysmal subarachnoid hemorrhage according to region, time period, blood pressure, and smoking prevalence in the population: a systematic review and meta-analysis. JAMA Neurol. 2019;76:588–97.
4. Kumar H, Ali S, Kumar J, et al. Dural venous sinus thrombosis leading to subarachnoid hemorrhage. Cureus. 2021;13:e13497.
5. Perillo T, Paolella C, Perrotta G, et al. Reversible cerebral vasoconstriction syndrome: review of neuroimaging findings. Radiol Med. 2022;127:981–90.
6. Viguier A, Raposo N, Patsoura S, et al. Subarachnoid and subdural hemorrhages in lobar intracerebral hemorrhage associated with cerebral amyloid angiopathy. Stroke. 2019;50:1567–9.
7. Edjlali M, Guédon A, Ben Hassen W, et al. Circumferential thick enhancement at Vessel Wall MRI has high specificity for intracranial aneurysm instability. Radiology. 2018;289:181–7.
8. Tateoka T, Yoshioka H, Kanemaru K, et al. Blood blister-like aneurysms at the junction of the internal carotid and posterior communicating artery: characteristics and treatment strategies. World Neurosurg. 2023;170:e645–51.
9. Hou K, Yu J. Current status of perimesencephalic non-aneurysmal subarachnoid hemorrhage. Front Neurol. 2022;13:960702.
10. Sacco S, Marini C, Toni D, et al. Incidence and 10-year survival of intracerebral hemorrhage in a population-based registry. Stroke. 2009;40:394–9.
11. Hemphill JC, Bonovich DC, Besmertis L, et al. The ICH score: a simple, reliable grading scale for intracerebral hemorrhage. Stroke. 2001;32:891–7.
12. Romero JM, Artunduaga M, Forero NP, et al. Accuracy of CT angiography for the diagnosis of vascular abnormalities causing intraparenchymal hemorrhage in young patients. Emerg Radiol. 2009;16:195–201.

13. Tranvinh E, Heit JJ, Hacein-Bey L, et al. Contemporary imaging of cerebral arteriovenous malformations. AJR Am J Roentgenol. 2017;208:1320–30.
14. Canedo-Antelo M, Baleato-González S, Mosqueira AJ, et al. Radiologic clues to cerebral venous thrombosis. Radiographics. 2019;39:1611–28.
15. Álvarez-Sabín J, Maisterra O, Santamarina E, et al. Factors influencing haemorrhagic transformation in ischaemic stroke. Lancet Neurol. 2013;12:689–705.
16. Jabbarli R, Reinhard M, Roelz R, et al. Intracerebral hematoma due to aneurysm rupture: are there risk factors beyond aneurysm location? Neurosurgery. 2016;78:813–20.
17. Li J, Jin M, Sun X, et al. Imaging of moyamoya disease and moyamoya syndrome: current status. J Comput Assist Tomogr. 2019;43:257–63.
18. Singhal AB, Hajj-Ali RA, Topcuoglu MA, et al. Reversible cerebral vasoconstriction syndromes: analysis of 139 cases. Arch Neurol. 2011;68:1005–12.
19. Abdel Razek AAK, Alvarez H, Bagg S, et al. Imaging spectrum of CNS vasculitis. Radiographics. 2014;34:873–94.
20. Koch MJ, Stapleton CJ, Guniganti R, et al. Outcome following hemorrhage from cranial dural arteriovenous fistulae: analysis of the multicenter international CONDOR registry. Stroke. 2021;52:e610–3.
21. in't Veld M, Fronczek R, Dos Santos MP, et al. High sensitivity and specificity of 4D-CTA in the detection of cranial arteriovenous shunts. Eur Radiol. 2019;29:5961–70.
22. Hefzy HM, Bartynski WS, Boardman JF, et al. Hemorrhage in posterior reversible encephalopathy syndrome: imaging and clinical features. AJNR Am J Neuroradiol. 2009;30:1371–9.
23. Walker DA, Broderick DF, Kotsenas AL, et al. Routine use of gradient-echo MRI to screen for cerebral amyloid angiopathy in elderly patients. AJR Am J Roentgenol. 2004;182:1547–50.
24. Charidimou A, Boulouis G, Frosch MP, et al. The Boston criteria version 2.0 for cerebral amyloid angiopathy: a multicentre, retrospective, MRI-neuropathology diagnostic accuracy study. Lancet Neurol. 2022;21:714–25.
25. Kranz PG, Malinzak MD, Amrhein TJ. Approach to imaging in patients with spontaneous intracranial hemorrhage. Neuroimaging Clin N Am. 2018;28:353–74.
26. Kuroedov D, Cunha B, Pamplona J, et al. Cerebral cavernous malformations: typical and atypical imaging characteristics. J Neuroimaging. 2023;33:202–17.
27. Steiner T, Weitz JI, Veltkamp R. Anticoagulant-associated intracranial hemorrhage in the era of reversal agents. Stroke. 2017;48:1432–7.